

Interface localized modes and hybrid lattice solitons in waveguide arrays

Mario I. Molina

*Departamento de Física, Facultad de Ciencias, Universidad de Chile, Casilla 653,
Santiago, Chile*

Yuri S. Kivshar

*Nonlinear Physics Center, Research School of Physical Sciences and Engineering,
Australian National University, Canberra ACT 0200, Australia*

We discuss the formation of guided modes localized at the interface separating two different periodic photonic lattices. Employing the effective discrete model, we analyze linear and nonlinear interface modes and also predict the existence of stable interface solitons including the *hybrid staggered/unstaggered lattice solitons* with the tails belonging to spectral gaps of different types. ©

2018 Optical Society of America

OCIS codes: 030.1640, 190.4420

Surface modes have been studied in different branches of physics including guided wave optics, where surface waves were predicted to exist at interfaces separating periodic and homogeneous dielectric media.¹ Recently, it was suggested theoretically² and demonstrated experimentally³ that nonlinearity-mediated trapping of light near the edge of a truncated waveguide array with self-focusing nonlinear response can lead to the formation of nonlinear localized surface states which can be understood as discrete optical solitons⁴ localized near and trapped by the surface⁵ for powers exceeding a certain threshold value. One of the important generalizations of these ideas is the concept of *multi-gap surface solitons*, i.e. mutually trapped surface states with components associated with different spectral gaps.⁶

In this Letter, we study another important generalization of the concept of nonlinear surface modes. We analyze linear and nonlinear optical guided modes localized at an interface separating two different semi-infinite periodic photonic lattices. In the framework of an effective discrete model we demonstrate that the analysis of linear interface states in such composite arrays provides an important tool for analyzing the interface solitons and their basic properties. We then find numerically the families of stable *interface lattice solitons* including a novel class of *hybrid staggered/unstaggered lattice solitons* with tails localized in spectral gaps of different types.

We consider an interface separating two different semi-infinite arrays of optical waveguides (as shown in the top of Fig. 1) described by the system of coupled-mode equations⁴ for the normalized mode amplitudes E_n :

$$i\frac{dE_n}{dz} + \epsilon_n E_n + (E_{n+1} + E_{n-1}) + \gamma|E_n|^2 E_n = 0, \quad (1)$$

where the propagation coordinate z is normalized to the intersite coupling V , E_n are defined in terms of the actual electric field \mathcal{E}_n as $E_n = (2V\lambda_0\eta_0/\pi n_0 n_2)^{1/2}\mathcal{E}_n$, λ_0 is the free-space wavelength, η_0 is the free-space impedance, n_0 and n_2 are the mean values of the linear and nonlinear refractive indices of each waveguide, and γ defines the nonlinear response strength. The waveguide interface is introduced by the condition: ϵ_0 at $n = 0$, and $\epsilon_n = \epsilon_A$ or $\epsilon_n = \epsilon_B$ for negative or positive n , respectively.

First, we look for *linear surface modes* in the form $E_n = A \xi_{\pm}^{|n|} \exp(i\beta z)$ localized near the interface waveguide with $n = 0$, and obtain the condition $\xi_+/\xi_- = \epsilon_{A0}/\epsilon_{B0}$ and the dispersion relation $\beta = \epsilon_0 + \frac{1}{2}(\epsilon_{A0} + \epsilon_{B0})(1 - \sqrt{1 + 4/\epsilon_{A0}\epsilon_{B0}})$, where $\epsilon_{A0} \equiv \epsilon_A - \epsilon_0$ and $\epsilon_{B0} \equiv \epsilon_B - \epsilon_0$. Figure 1 summarizes our results for the existence of such localized states on the parameter plane $(\epsilon_{A0}, \epsilon_{B0})$, as well as displays examples of localized modes corresponding to different existence regions. We note the existence of two sectors where no localized states exist (shaded regions). One of them is bounded by the curves $\epsilon_{B0} = 4/|\epsilon_{A0}|$ (for $-\infty < \epsilon_{A0} < 0$) and $\epsilon_{B0} = \epsilon_{A0}/(1 - \epsilon_{A0})$ (for $-\infty < \epsilon_{A0} < 1$). The other one is obtained by a reflection across the origin. Inside these regions either $|\xi_{+1}|$, $|\xi_{-1}|$ or both exceed one.

One of the important observations that follows from our analysis is the existence of *hybrid staggered/unstaggered interface modes* for the opposite sign of the propagation constant mismatches of two lattices. These modes have the tails localized in the bandgaps of different types, i.e. above (for one array) and below (for the other array) of the spectral band.

In Figs. 2(a,b) we show the propagation constant β of the localized modes as a function of the interface parameter ϵ_0 , for the characteristic cases (a) $\epsilon_A = 0.6$, $\epsilon_B =$

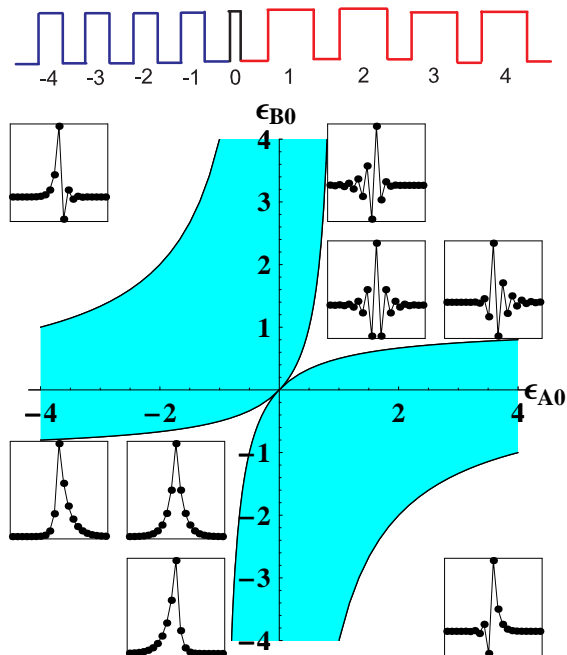


Fig. 1. (Color online) Phase diagram of different types of localized interface modes. No localized modes exist inside the shaded areas. The insets show examples of localized modes corresponding to different values of $\epsilon_{A0} \equiv \epsilon_A - \epsilon_0$ and $\epsilon_{B0} \equiv \epsilon_B - \epsilon_0$. Top: schematic structure of the waveguide interface.

-0.6 , and (b) $\epsilon_A = 3, \epsilon_B = -3$. We note that the mode always lies outside the linear spectral bands, but its structure depends strongly on the overlap of the bands, so that the hybrid modes appear for a relatively large band mismatch, as shown in Fig. 2(b) (middle curve).

The analysis of linear localized interface modes in such an array provides an important information about the existence of nonlinear interface modes—*lattice surface solitons*. Next, we consider two semi-infinite nonlinear waveguide arrays character-

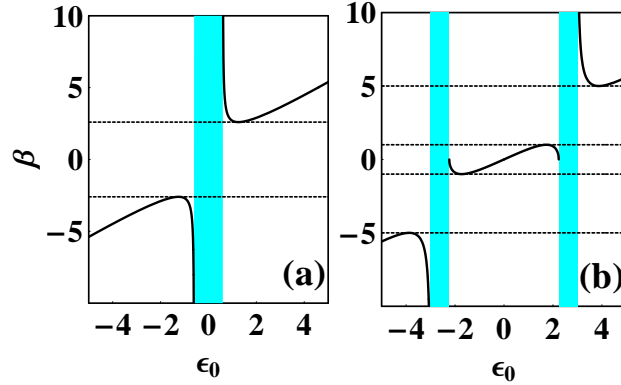


Fig. 2. (Color online) Families of localized modes shown as the dependencies β vs. ϵ_0 , for the cases: (a) $\epsilon_A = 0.6, \epsilon_B = -0.6$, and (b) $\epsilon_A = 3, \epsilon_B = -3$. No localized modes exist inside the shaded regions. The dashed lines mark the spectral bands of both arrays, which in the case (b) do not overlap with each other.

ized by propagation constants ϵ_A and ϵ_B that are joined by an interface waveguide with the propagation constant ϵ_0 . We focus on the interface modes defined by having their centers at either the first of the A waveguides or the first of the B waveguides. We find different classes of nonlinear localized modes and study their linear stability numerically via a multidimensional Newton-Raphson method.

First, we consider the case $\epsilon_0 = \epsilon_A = -\epsilon_B = 0.6$ and $\gamma = +1$. In the linear limit, this corresponds to a negative vertical line in Fig. 1, where no localized modes exist. The presence of nonlinearity shifts the propagation constant of the mode to the left, until it gives rise to an unstaggered localized mode. Therefore, we predict the lowest nonlinear interface mode to be unstaggered. This is indeed confirmed by our numerical

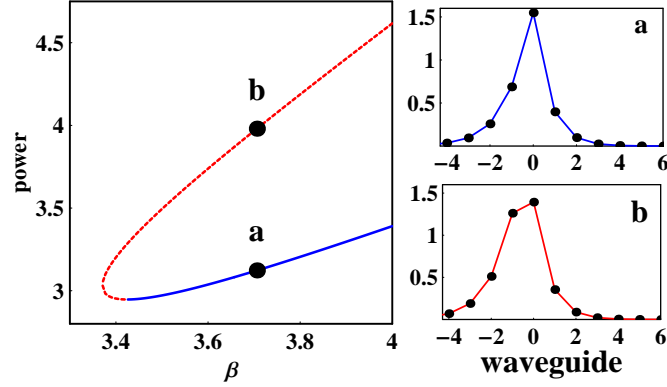


Fig. 3. (Color online) Power vs. propagation constant for the interface unstag-gered solitons centered on the first A waveguide (for $\epsilon_A = \epsilon_0 = 0.6$, $\epsilon_B = -0.6$). The solid (dashed) curve refers to the stable (unstable) branches. Inserts show two examples of the interface modes.

computations, and the family of the lowest-order interface nonlinear modes is shown in Fig. 3, where the upper/lower branch corresponds to unstable/stable modes. Next, we consider the case $\epsilon_A = 3$, $\epsilon_0 = 0$ and $\epsilon_B = -3$. Results are summarized in Fig. 4 which shows the dependence of the power vs. propagation constant for several low-power modes. We note that the lowest mode extends all the way to zero power, and therefore it corresponds in that limit to the linear mode induced by three concurrent dissimilar propagation constants. More importantly, the mode amplitudes show now a *hybrid character*, being unstaggered in one side of the interface and staggered on the other.

In addition, we find many other types of nonlinear interface modes including twisted and flat-top modes, as well as the modes with different location of their

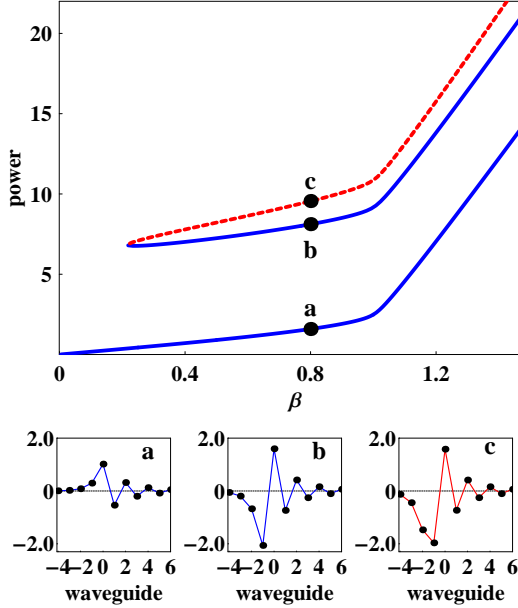


Fig. 4. (Color online) Power vs. propagation constant for the hybrid interface staggered/unstaggered lattice solitons for $\epsilon_A = -3, \epsilon_0 = 0, \epsilon_B = 3$. Solid (dashed) curves refer to the stable (unstable) branches. Inserts show three examples of the hybrid interface solitons.

centers relative to the interface, as discussed earlier for a semi-infinite waveguide array.⁵ As a special limit of those modes, we find also the *kink surface modes* which are extended in one direction while being localized in the other.

Next, we study the evolution of all types of nonlinear interface modes checking in this way our stability results and analyzing the evolution scenario for the unstable modes. In all cases examined, we observe that the unstable modes decay into the unstaggered fundamental

mode by emitting radiation. In particular, for the unstaggered unstable modes, this decay is rapid and it proceeds vertically. For other cases, the unstable localized

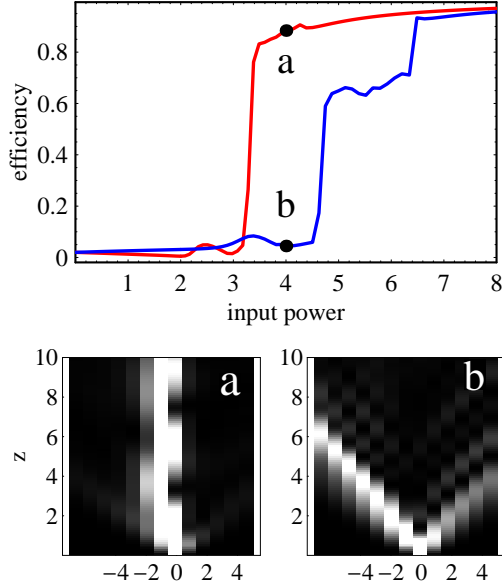


Fig. 5. (Color online) Top: trapping efficiency for the generation of interface solitons. The red (blue) curve denotes the case when the initial input is centered on the first A (B) waveguide. Bottom: evolution of initial states marked ‘a’ and ‘b’ (for $\epsilon_A = 0.6$, $\epsilon_B = -0.6$).

modes decay into higher-power generalizations of the fundamental mode. Also, we observe that unstable unstaggered modes decay much faster than unstable twisted, flat-top, or dark-like nonlinear modes.

Finally, we study how an interface lattice soliton can be generated in experiment by exciting a single waveguide which is either the very first of the A waveguides, or the very first of the B waveguides. We define the trapping efficiency as the power fraction $P_{\text{out}}/P_{\text{in}}$ remaining in the 10 central waveguides. Results for the trapping efficiency are shown in Fig. 5(top), where we have used 201 waveguides, a total evolution length of 20. The bottom portion of Fig. 5 shows the evolution of the initial states marked

by the points ‘a’ and ‘b’ in Fig. 5(top).

We would like to emphasize that the results obtained here can be easily generalized to the case of *surface gap solitons* which were predicted theoretically⁷ and observed experimentally⁸ in periodic photonic lattices with defocusing nonlinearity, where surface solitons appear in the gaps of the photonic bandgap spectra or their overlaps.

In conclusion, we have analyzed different types of linear and nonlinear optical guided modes localized at the interface separating two different semi-infinite periodic photonic lattices. In the framework of an effective discrete nonlinear model, we have demonstrated the existence of stable interface lattice solitons including the hybrid staggered/unstaggered discrete solitons with the tails that belong to different spectral gaps. We believe our results will encourage the first experimental observations of this novel type of surface optical solitons in photonic lattices.

This work has been supported by Conicyt and Fondecyt grants 1050193 and 7050173 in Chile, and by the Australian Research Council in Australia.

References

1. P. Yeh, A. Yariv, and A.Y. Cho, *Appl. Phys. Lett.* **32**, 102 (1978).
2. K.G. Markis, S. Suntsov, D.N. Christodoulides, G.I. Stegeman, and A. Haché, *Opt. Lett.* **30**, 2466 (2005).
3. S. Suntsov, K.G. Markis, D.N. Christodoulides, G.I. Stegeman, A. Haché, R. Morandotti, H. Yang, G. Salamo, and M. Sorel, *Phys. Rev. Lett.* **96**, 063901 (2006).

4. Yu.S. Kivshar and G.P. Agrawal, *Optical Solitons: From Fibers to Photonic Crystals* (Academic, San Diego, 2003), and references therein.
5. M. Molina, R. Vicencio, and Yu.S. Kivshar, *Opt. Lett.* **31**, 1693 (2006).
6. I.L. Garanovich, A.A. Sukhorukov, Yu.S. Kivshar, and M. Molina, *Opt. Express* **14**, 4780(2006).
7. Ya.V. Kartashov, V.A. Vysloukh, and L. Torner, *Phys. Rev. Lett.* **96**, 073901 (2006).
8. C.R. Rosberg, D.N. Neshev, W. Krolikowski, A. Mitchell, R.A. Vicencio, M.I.Molina, and Yu.S. Kivshar, *Phys. Rev. Lett.* **97**, 083901 (2006).

List of Figure Captions

Figure 1: (Color online) Phase diagram of different types of localized interface modes. No localized modes exist inside the shaded areas. The insets show examples of localized modes corresponding to different values of $\epsilon_{A0} \equiv \epsilon_A - \epsilon_0$ and $\epsilon_{B0} \equiv \epsilon_B - \epsilon_0$. Top: schematic structure of the waveguide interface.

Figure 2: (Color online) Families of localized modes shown as the dependencies β vs. ϵ_0 , for the cases: (a) $\epsilon_A = 0.6, \epsilon_B = -0.6$, and (b) $\epsilon_A = 3, \epsilon_B = -3$. No localized modes exist inside the shaded regions. The dashed lines mark the spectral bands of both arrays, which in the case (b) do not overlap with each other.

Figure 3: (Color online) Power vs. propagation constant for the interface unstaggered solitons centered on the first A waveguide (for $\epsilon_A = \epsilon_0 = 0.6, \epsilon_B = -0.6$). The solid (dashed) curve refers to the stable (unstable) branches. Inserts show two examples of the interface modes.

Figure 4: (Color online) Power vs. propagation constant for the hybrid interface staggered/unstaggered lattice solitons for $\epsilon_A = -3, \epsilon_0 = 0, \epsilon_B = 3$. Solid (dashed) curves refer to the stable (unstable) branches. Inserts show three examples of the hybrid interface solitons.

Figure 5: (Color online) Top: trapping efficiency for the generation of interface solitons. The red (blue) curve denotes the case when the initial input is centered on the first A (B) waveguide. Bottom: evolution of initial states marked ‘a’ and ‘b’ (for $\epsilon_A = 0.6, \epsilon_B = -0.6$).